Master's Thesis

UnaG, a Photoswitchable Fluorogen-Binding Protein for STORM (STochastic Optical Reconstruction Microscopy) Imaging

Gyeong Tae Kim

Department of Biomedical Engineering

Graduate School of UNIST

2017

UnaG, a Photoswitchable Fluorogen-Binding Protein for STORM (STochastic Optical Reconstruction Microscopy) Imaging

Gyeong Tae Kim

Department of Biomedical Engineering

Graduate School of UNIST

UnaG, a Photoswitchable Fluorogen-Binding Protein for STORM (STochastic Optical Reconstruction Microscopy) Imaging

A thesis/dissertation
submitted to the Graduate School of UNIST
in partial fulfillment of the
requirements for the degree of
Master of Science

Gyeong Tae Kim

12. 12. 2016
Approved by

Advisor
Sung Chul Bae

UnaG, a Photoswitchable Fluorogen-Binding Protein for STORM (STochastic Optical Reconstruction Microscopy) Imaging

Gyeong Tae Kim

This certifies that the thesis/dissertation of Gyeong Tae Kim is approved.

12/12/2016

signature

Advisor: Sung Chul Bae

signature

Sung Chul Bae: Thesis Committee Member #1

signature

Hajin Kim: Thesis Committee Member #2

signature

Chung Hun Park: Thesis Committee Member #3

Abstract

STORM (STochastic Optical Reconstruction Microscopy), which offers an order of magnitude improvement in resolution, is based on high-precision single-molecule localization of photoswitchable fluorophores. The performance of STORM depends on photophysical properties of photoswitching fluorophores. Conventional fluorescent proteins used in STORM suffer from fast photobleaching, which results in limited number of independent snapshots in live-cell super-resolution imaging. We aim to develop a new STORM fluorophore for virtually no photobleaching. UnaG, a fluorogen-binding protein derived from the Japanese freshwater eel, fluoresces upon binding of non-fluorescent bilirubin, an endogenous metabolite.

We discovered photoswitching behavior of UnaG; UnaG fluorescence turns off upon 488-nm illumination. The photoswitching of UnaG can be repeated about hundreds of switching cycle. Most notably, we found that UnaG fluorescence recovers after photobleaching when exogenous bilirubin is added into the imaging buffer solution. We have applied UnaG to STORM imaging of the subcellular ultrastructure.

Contents

Figure Contents

Ⅰ. Introduction

Fluorescence microscopy has provided biology research with advanced opportunities for imaging with high biochemical specificity. However, it has one big challenge which is diffraction limit proposed by Abbe so that cannot image ultrastructure of cellular construction. There are some approaches to solve the diffraction limit[1]-[4]. Super-resolution microscopy is the way to solve it through spatial or temporal modulation of fluorophores. There are some approaches including stimulated emission depletion (STED) [3], structured-illumination microscopy (SIM) [2], and photo-activation localization microscopy (PALM) [4] or stochastic optical reconstruction microscopy (STORM) [1].

In this study, we have used STORM which depends on randomly turning on and off of switching fluorophores. STORM image is reconstructed from high accuracy localization of each fluorophore that are randomly switched on and off[1]. The reconstruction process consists of overlapping of series of cycles (Fig. 1). In each cycle, the position of stochastically switching fluorophores are determined with high accuracy localization algorithm based on Gaussian distribution. After repeating enough these cycles, overlapping overall localization provides reconstructed super-resolution STORM image, which resolution could be near 20 nm[5].

Despite of this advantage, they have faced high-laser dose and photobleaching of fluorophores that inhibits long time-lapse imaging of biological samples[6][7]. The photobleaching is the permanently destruction of fluorophore structure and biology samples are sensitive to the laser dose that is harmful to cellular condition[8]. These problems come from high laser usage of currently used super-resolution imaging techniques[8]-[11].

Recently, fluorescent proteins from vertebrates, called UnaG, was introduced[12]. One of characteristics of the fluorescent protein is that it is ligand-activated fluorophore and switching[13]. UnaG fluorescence is triggered by an endogenous metabolite, bilirubin. After switching off of the fluorescence, UnaG could recover its fluorescence with bilirubin. By using this sense, we assume it could be alternative fluorophore which can free from photobleaching in exogenous bilirubin buffer condition.

In this study, we used the UnaG for mammalian imaging fluorophore for STORM especially for long time-lapse STORM imaging. We identified the photophysical properties of UnaG to estimate proper STORM imaging condition. Then we did transfect UnaG to ER, mitochondria, and vimentin to perform actual STORM imaging.

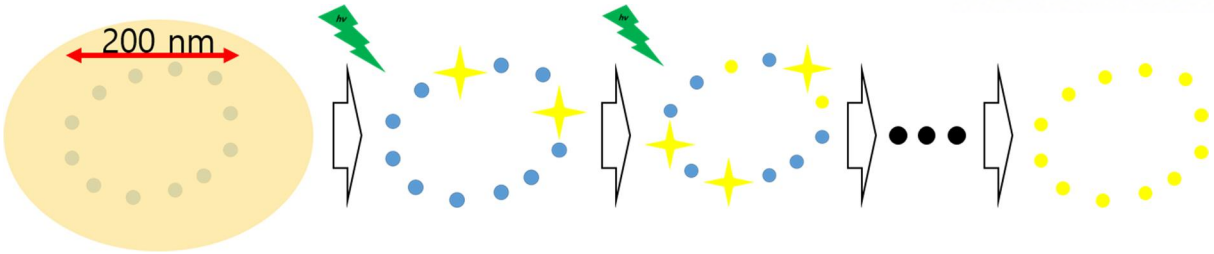

Figure 1. A STORM imaging cycle of photoswitchable fluorophores.

Because of diffraction limit, the object is seen like beige-colored shape (left) with conventional microscopy. Under suitable light dose, stochastic subset of fluorophores (blue) switched on and off (yellow) with high accuracy localization. After enough repeating of the cycles and then overlapping all localization data provide super-resolution STORM image (right).

Ⅱ. Experimental Method and Materials

2.1. Fluorescence Microscope

We have used commercial microscopy for video rate single-molecule localization, which is Vutara SR-350 (Bruker) (Fig. 2). A 60x oil immersion objective lens (Olympus). And sCMOS camera (Hamamatsu) of 6.5 um x 6.5 um pixel size for super-resolution imaging was used for super-resolution imaging. A CCD camera which has 1392x1040 was used for widefield imaging. Vutara SR-350 has Fully motorized XY scanning stage. Objective-mounted piezo for Z focus within 100 um depth was equipped. Total Internal Reflection Fluorescence (TIRF) mode was also available. 3 lasers (561-nm, 488-nm, 405-nm) were used for excitation and activation source. Filter wheels equipped 2 multi-band pass filter was located in emission path.

Figure 2. Vutara SR-350 (Bruker) for STORM imaging.

2.2. Image Analysis

Real time image analysis and post-processing were performed by using SRX Software, which also could control all devices of Vutara SR-350 (Fig. 3). It utilized single molecule localization to circumvent the diffraction limit of light by randomly activating and deactivating a sparse, isolated subset of fluorophores within a sample.

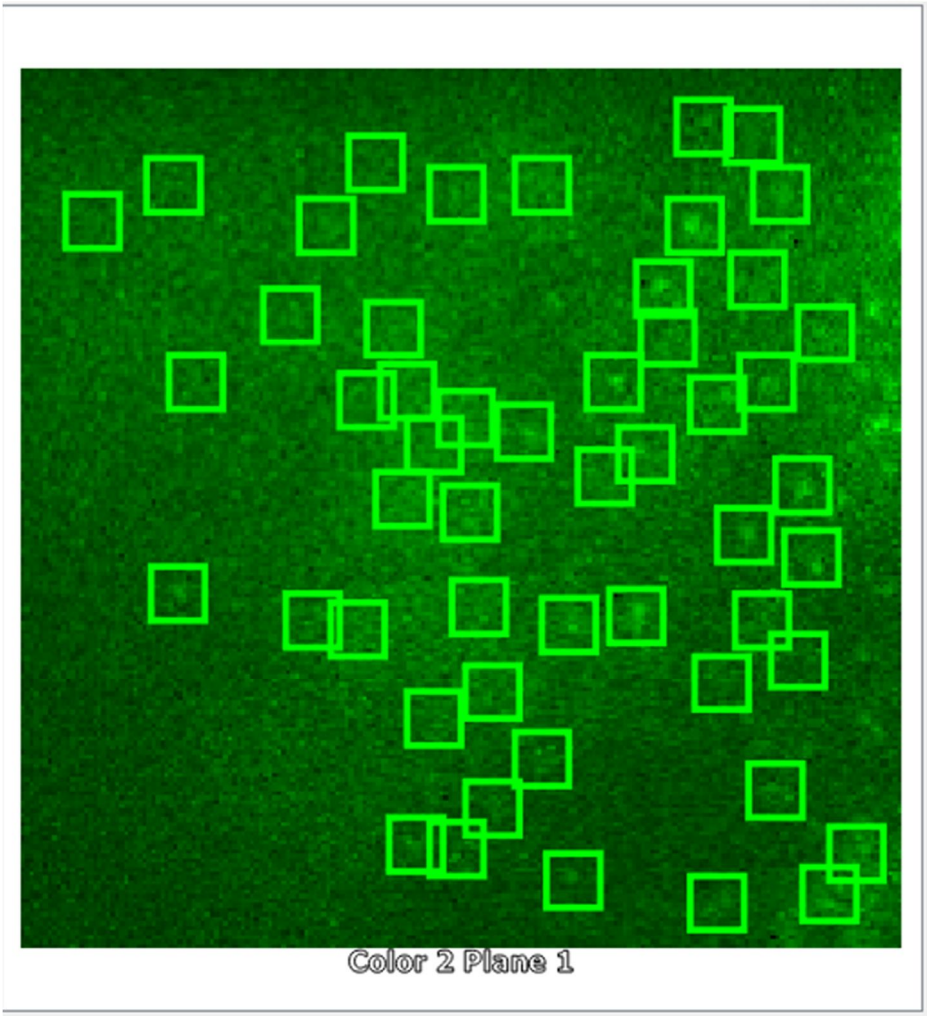

Figure 3. SRX software for real-time localization process of STORM.

2.3. Cell Culture

U2-OS cells were maintained in a 5 % CO_2 and 37 °C in a McCoy (Gibco) supplemented with 10 % FBS, 50 unit/mL penicillin, and 50 μg/mL streptomycin.

COS7 cells, an African green monkey kidney cell line, and HEK-293T cells were maintained in a 5 % CO_2 and 37 °C in Minimum Essential Medium (Gibco) supplemented with Fetal Bovine Serum (FBS) 10 %, 50 units/mL penicillin, and 50 μg/mL streptomycin.

All Cells were passaged 2~3 days and grown up to 20 passages. Cells were grown on 18 mm round cover slips in a 12 well plate.

2.4. Transfection

Live cells were transfected at 60~80% confluence. 5 μL of Lipofectamine 2000 (Life Technologies) and 1,000 ng plasmid per well were used for transfection.

2.5. Fixation

Cells expressing UnaG were fixed with 4 % paraformaldehyde in Dulbecco's Phosphate Buffered Saline (DPBS) at room temperature for 15 min. Then washed three times with DPBS and permeablized with 0.4 % Triton X100 at room temperature for 1 hour. Cells were washed three times with DPBS and blocked with 2 % BSA in DPBS at room temperature for 1 hour.

2.6. Staining

For staining of mitochondria, transfected cells were incubated in 0.2~0.5 μM MitoTracker Red (Invitrogen) in Dulbecco's Modified Eagle Medium (DMEM) for 30 seconds, and then washed three times with DMEM.

2.7. Imaging Buffer

Imaging buffer was prepared with Phosphate Buffered Saline (PBS) supplemented with 2% glucose, oxygen scavenger (0.5 mg/mL glucose oxidase and 40 μg/mL catalase), and 500 nM bilirubin before imaging.

Ⅲ. Results

3.1. UnaG Photophysical Properties

To estimate photoswitching property of UnaG, the conformational change of bilirubin, which can be reversible complex with UnaG, need to be demonstrated. Bilirubin indirectly breaks down heme in vertebrates in normal catabolic pathway. It is reported that bilirubin undergoes conformational change through light illumination and oxidation process (Fig. 4) [14]. UnaG could make very specific selectivity and binding affinity (K_d = 98 pM) with bilirubin while other bilirubin related compounds could not[13]. The apo-UnaG and bilirubin, both are non-fluorescent construct, have fluorescence when they are binding form, called holo-UnaG. 498 nm light illumination to holo-UnaG causes 527 nm light emission[14]. In this process conformational changed bilirubin detached from holo-UnaG and it turns back to apo-UnaG (switch off). We assume the switching model of UnaG briefly like in Figure 5 and check the actual switching of UnaG by using purified UnaG protein (Fig. 6). The 200 mM of apo-UnaG did not fluorescent with 488 nm laser dose. Through 1mM bilirubin addition, UnaG emitted green fluorescence. UnaG lost fluorescence due to conformational change of bilirubin through continuous exposure with laser and oxygen. Addition of fresh bilirubin turns on UnaG again.

The switching cycle and fluorescent endurance was also measured during cell imaging (Fig. 7). The fixed U2-OS cells expressing UnaG-mito were used for measurement. With 20mW of 488 nm laser

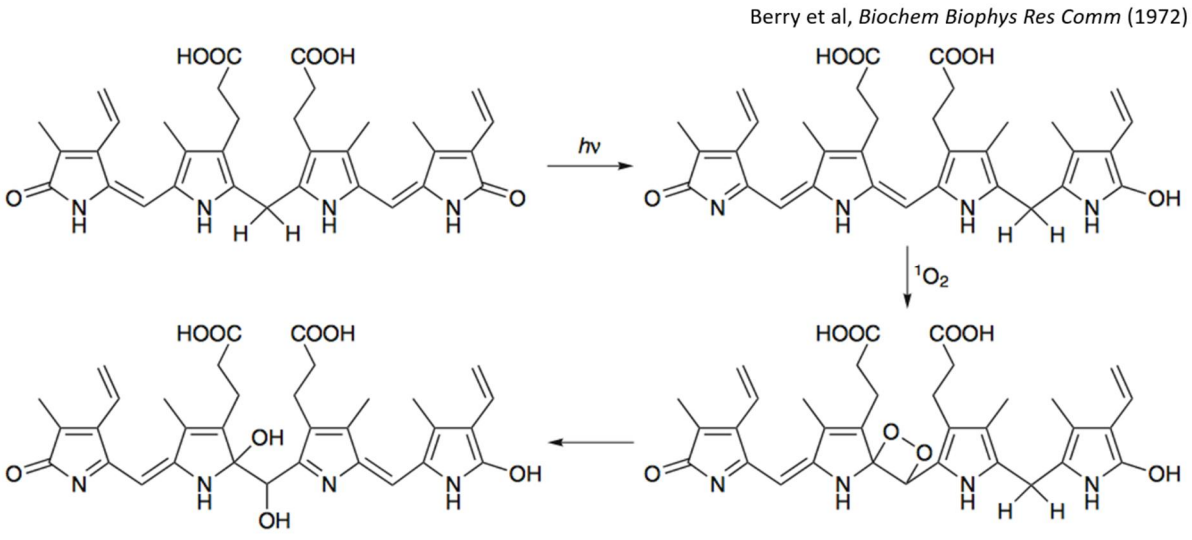

Figure 4. Chemical structure and reaction of bilirubin.

Bilirubin undergoes structural changes under exposure to the light and then singlet oxygen. This process is irreversible mechanism.

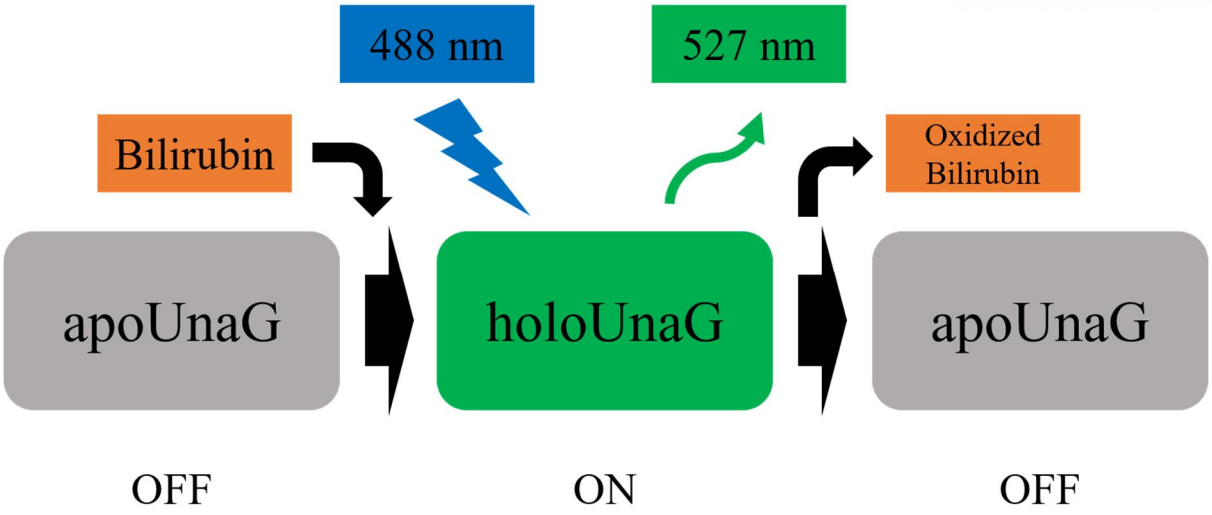

Figure 5. Brief switching mechanism of UnaG.

Non-fluorescent apoUnaG combined with bilirubin and then becomes fluorescent holoUnaG. The holoUnaG is excited with 488 nm illumination and emits 527 nm fluorescence. During switch-off mechanism, oxidized bilirubin is detached and UnaG turns back to non-fluorescent UnaG.

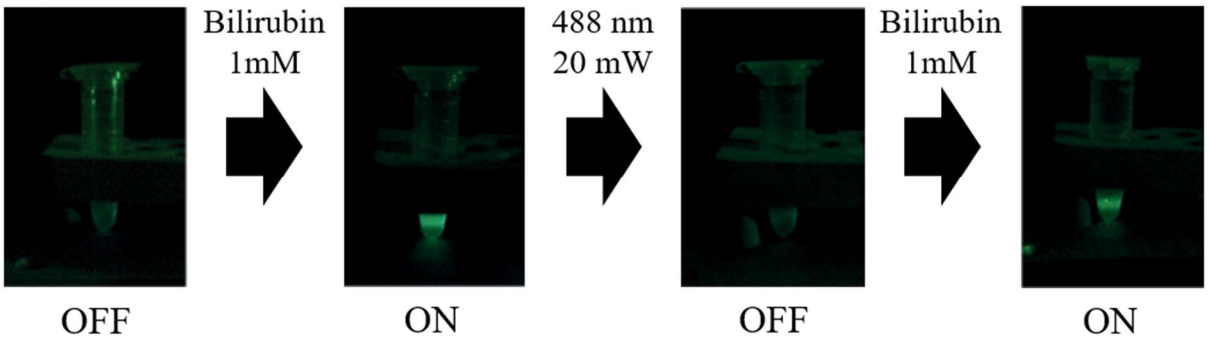

Figure 6. Switching ON and OFF of UnaG.

Purified 200mM of holo-UnaG was measured with 488 nm laser until UnaG fluorescence turns off. Then fresh bilirubin was added to the same tube. After checking fluorescence turns back on with 488 nm laser illumination, 20mW 488 nm laser illuminate tube again until all fluorescence turn off. The fluorescence was captured with 530/55 filter.

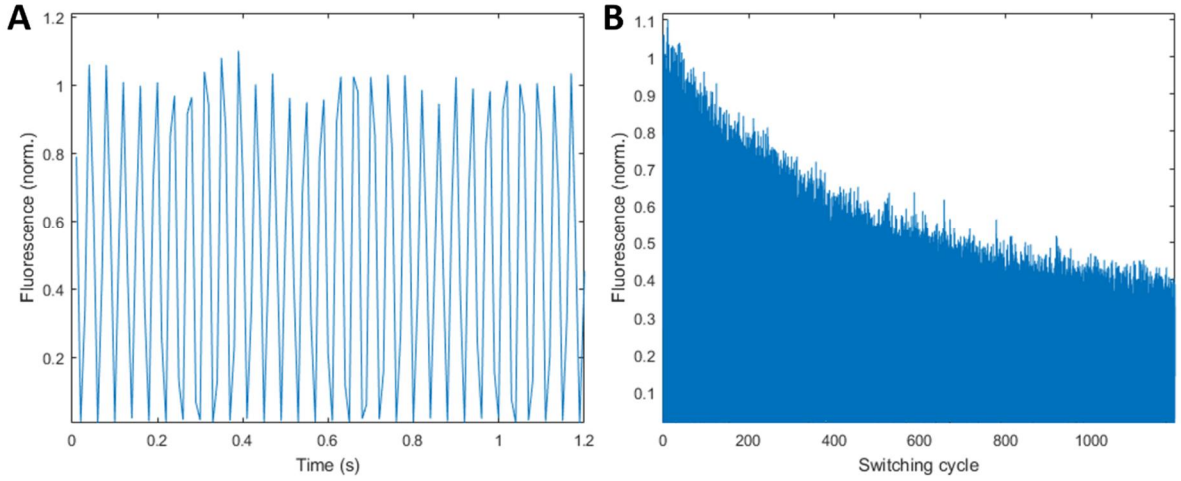

Figure 7. Switching cycle measurement of UnaG.

(A) Fluorescent intensity of UnaG expressed U2-OS cell illuminated with 488 nm laser. Switching frequency was 25 Hz. Measuring EMCCD camera rate was 200 Hz. (B) About 700 cycles are measured until fluorescence decreases at half of intensity.

illumination and 200 Hz shutter speed of EMCCD camera setting, a series of images were captured during 2 seconds. By analyzing fluorescence of small ROI on the mitochondria in all acquired images, switching molecule speed could be measured. The switching cycle of UnaG was 25 Hz (Fig 7. A) and it was enough cycle speed compared with other photoswitchable green fluorescent proteins[15]-[18]. The number of cycles until initial fluorescent intensity decreased about half was also measured with same results. About 700 cycles were measured to reach decreasing half of fluorescent intensity (Fig 7. B). However, its duty could be longer by adding exogenous bilirubin because oxidized bilirubin change position with bilirubin and then recover fluorescence of UnaG. Continuous cell images show the fluorescence recovery of UnaG. With bilirubin-rich imaging buffer, fixed U2-OS cells expressing UnaG-mito were imaged by using confocal microscopy. First cells were exposure with weak 488 nm laser to prevent from fast switch off. After capturing first image, increased laser intensity caused photobleaching of UnaG. Then same ROI of the cell was continuously imaged (Fig. 8). The fluorescence of UnaG was slowly recovered and recovered almost same amount of initial fluorescence after 10 minutes.

To study more about switching pattern of UnaG, we tested it with various condition. The 200 nM of holo-UnaG was illuminated with various 488 nm laser intensity to examine off-switching pattern (Fig. 9). The fluorescence decreasing ratio linearly depended on the laser intensity. With 80mW/cm2 of 488 nm laser, fluorescence of UnaG was fastly decreased without oxygen scavanger while fluorescence was

slowly decreased with oxygen scavanger. The fluorescence of UnaG lasted under oxygen scavanger system so that maintaining of low oxygen concentration in imaging buffer was important to perform long time-lapse STORM imaging.

We also tested on-switching behavior of UnaG to study relation with bilirubin (Fig. 10). The amount of fluorescent recovery was increased with bilirubin concentration.in solution. Because the increasing trend was not linear, on-switching coefficient had two kinds of reaction coefficients through fitting. The UV activation possibility was also examined. The result show UnaG did not activated its fluorescence by UV.

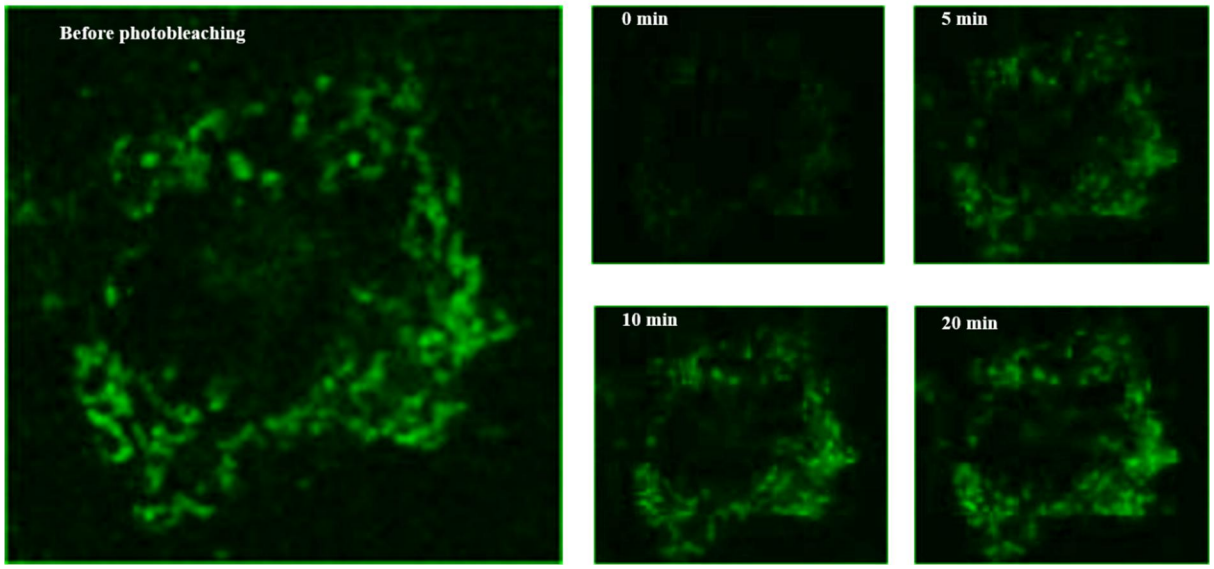

Figure 8. Fluorescence recovery of UnaG.

UnaG-mito pattern was shown well with weak 488 nm laser. After photobleaching, fluorescence of UnaG was recovered due to combine with fresh bilirubin as time goes on. The fluorescence was fully recovered in 20 minutes after photobleaching.

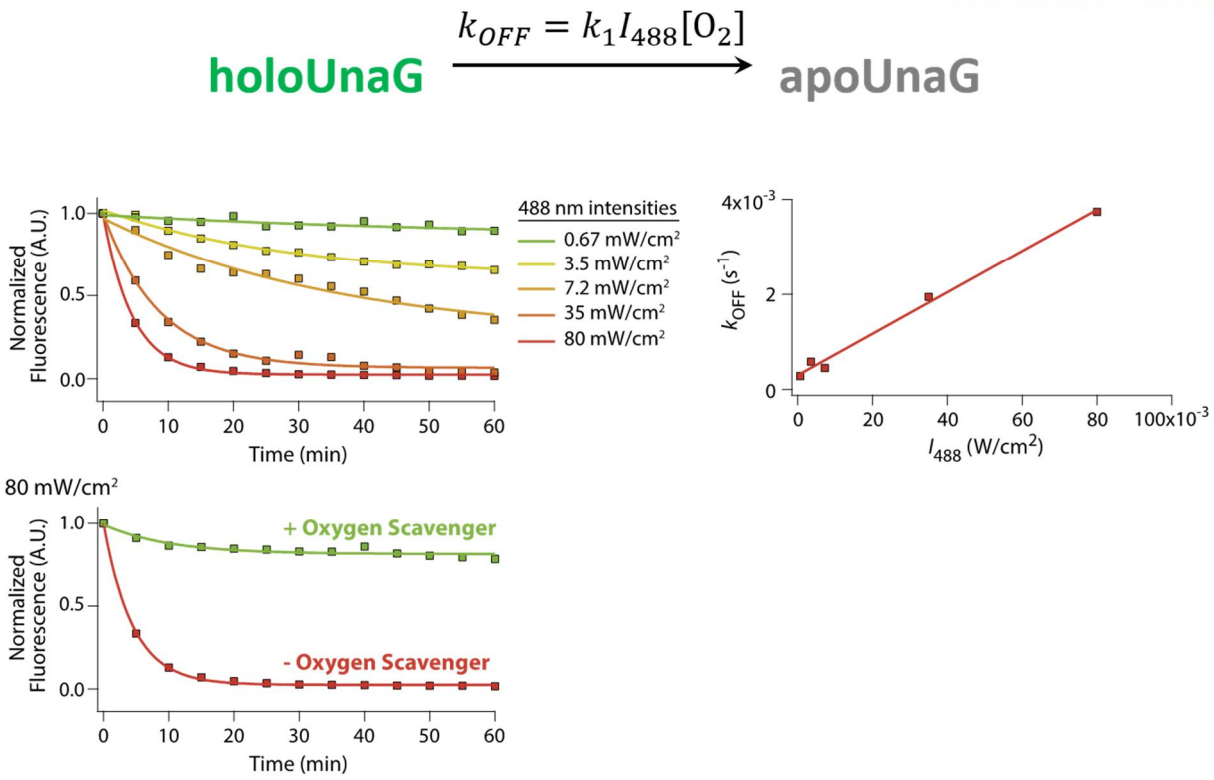

Figure 9. Off-switching behavior of UnaG.

A fluorescence intensity of the holoUnaG depended on 488 nm laser intensity and the fluorescent increasing trend show linear graph. UnaG was also affected by oxygen concentration in solution. In low oxygen atmosphere, the fluorescence of UnaG was decreased much slower than normal oxygen concentration solution.

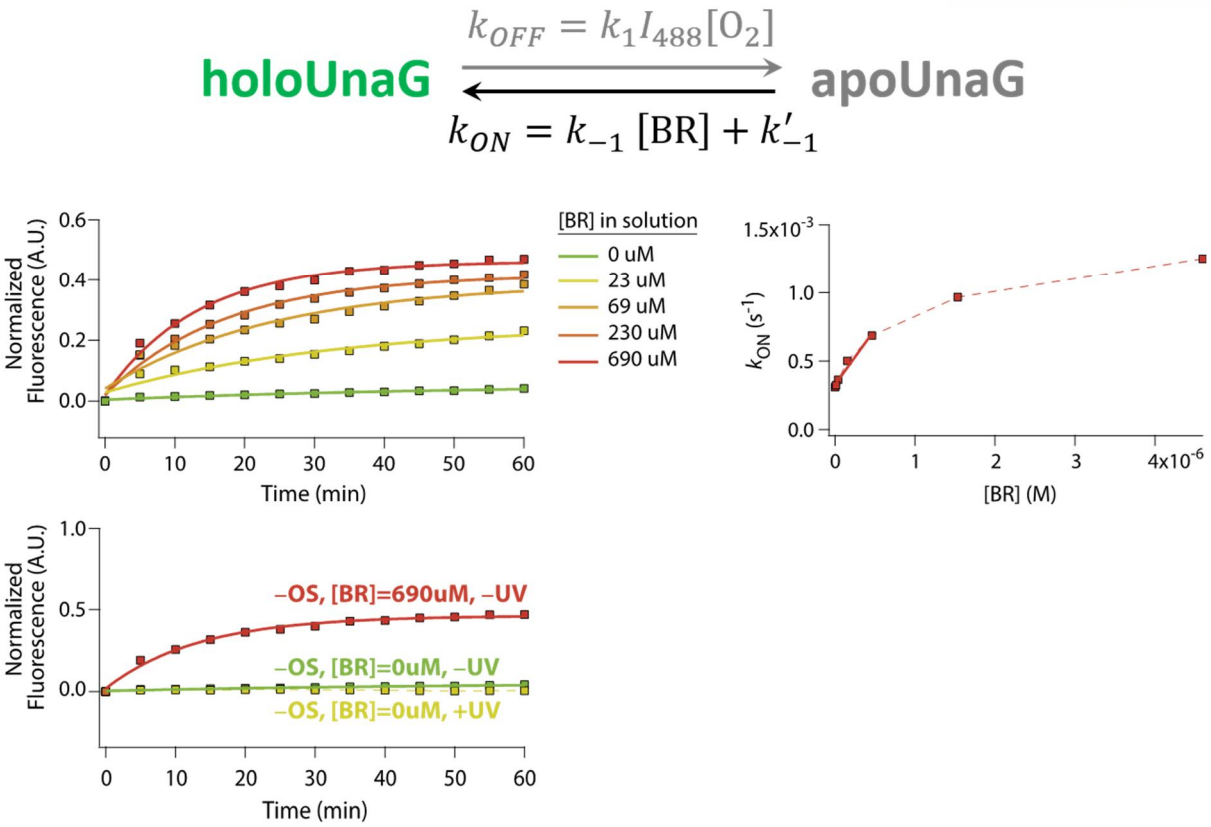

Figure 10. On-switching behavior of UnaG.

The fluorescence of UnaG turned on with bilirubin and the amount of fluorescent recovery depended on the bilirubin concentration. A relation between UnaG and bilirubin show not linear trend rather logarithm shape. UnaG was not activated by UV illumination.

3.2 Live Cell STORM Imaging for UnaG

Based on the photophysical properties of UnaG, we found proper STORM imaging condition. We used COS7 cells expressed with various UnaG construct. The sec61β is one of family of ER membrane protein translocator[19]. UnaG was fused with the sec61β, which was UnaG-sec61β. We attempted to perform STORM image with the UnaG construct (Fig. 11). Under weak 488 nm excitation (3 mW), UnaG fluorescence switched on and off. We used PBS based imaging buffer including bilirubin,

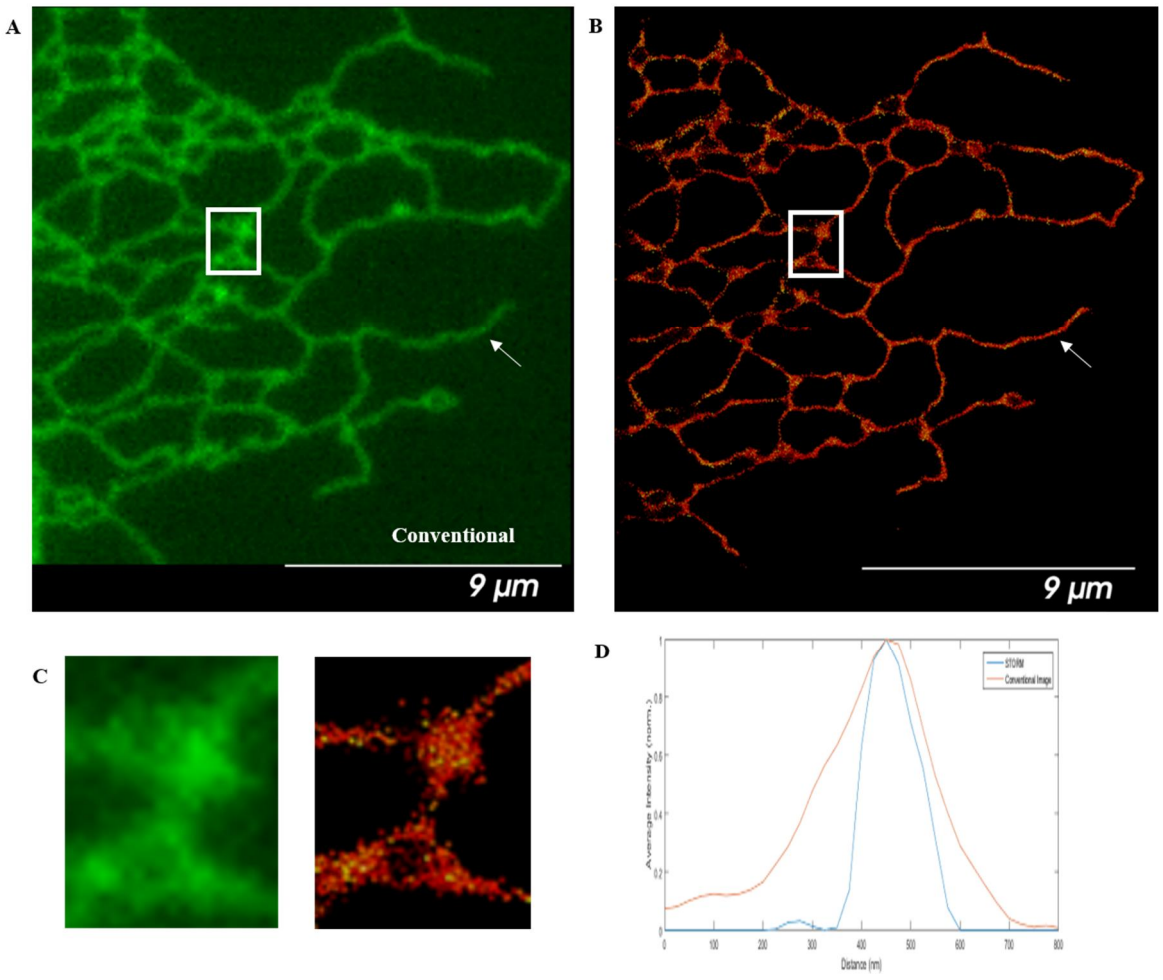

Figure 11. STORM images with a live COS7 cell expressing UnaG-sec61β.

Conventional image (A) and STORM image (B). White arrows on (A) and (B) indicate the cross sectional region to compare thickness between STORM image and conventional image. (C) Zoom inside of boxed regions of A (left) and B (right). (D) Thickness profile graph show STORM image has 2 times smaller FWHM than conventional image. Scale bar size is 9 μm.

glucose and GLOX (oxygen scavenger). Resulted STORM image (Fig. 11. A) show enhanced resolution than conventional image (Fig. 11. B). The thickness profile of ER tubule show STORM image show 2 times better resolution than conventional image from 300 nm to 150 nm (Fig. 11. D).

We also performed STORM imaging with another construct, vimentin, which has important role to support and anchor the structure in the cytosol (Fig. 12). Imaging condition was same with UnaG-sec61 β STORM.

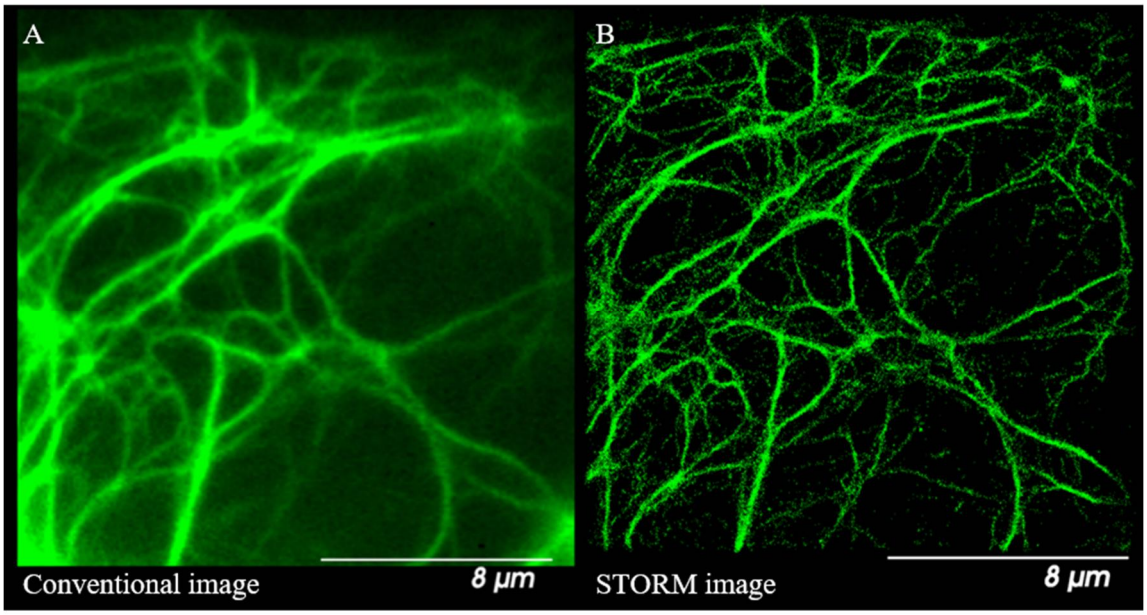

Figure 12. Vimentin-UnaG STORM image of fixed COS7 cell.

Conventional image (A) and STORM image (B) of fixed COS7 cell expressing Vimentin-UnaG. STORM image show the detail tubule image than conventional image. Scale bar size is 8 μm.

We performed STORM imaging for long time-lapse with UnaG-sec61β and UnaG-mito, which expressing mitochondria membrane. STORM imaging for the two construct was performed with same imaging condition, 3 mW 488 nm laser and 10 msec of sCMOS camera frame rate. Imaging buffer condition was also same with previous STORM imaging. We made one STORM imaging by using 1000 frames of individual images. STORM imaging was continuous longer than 100 minutes. The conventional images show almost same fluorescent intensity at that time (Fig. 13). There were a lot of movements of ER during 100 minutes. The continuous STORM images composed of 1000 low images

were acquired longer than 100 minutes (Fig. 14). We also performed long time-lapse STORM image with UnaG-mito construct. Each STORM images were composed of 1000 frames of low images (Fig 15). STORM imaging were continued over 350 seconds.

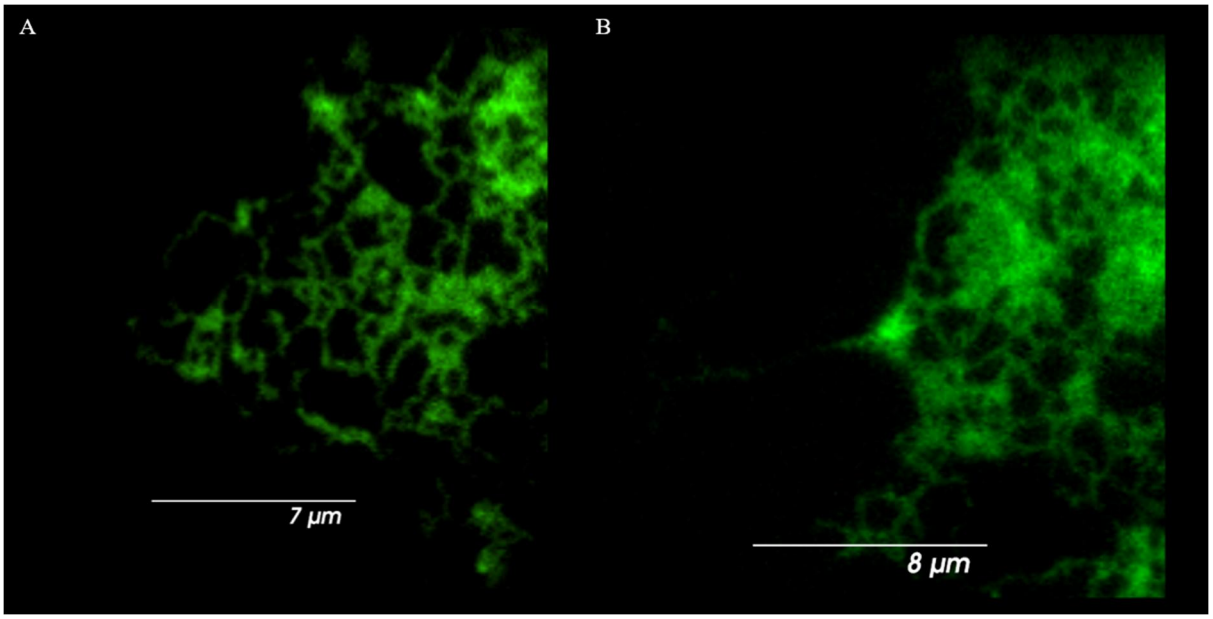

Figure 13. Fluorescence of UnaG lasts until 100 minutes after continuous STORM imaging.
(A) The first conventional level image of UnaG-sec61β and conventional image of same ROI after 100 minutes with continuous STORM imaging. During 100 minutes, a lot of ER mitochondria dynamics occurred.

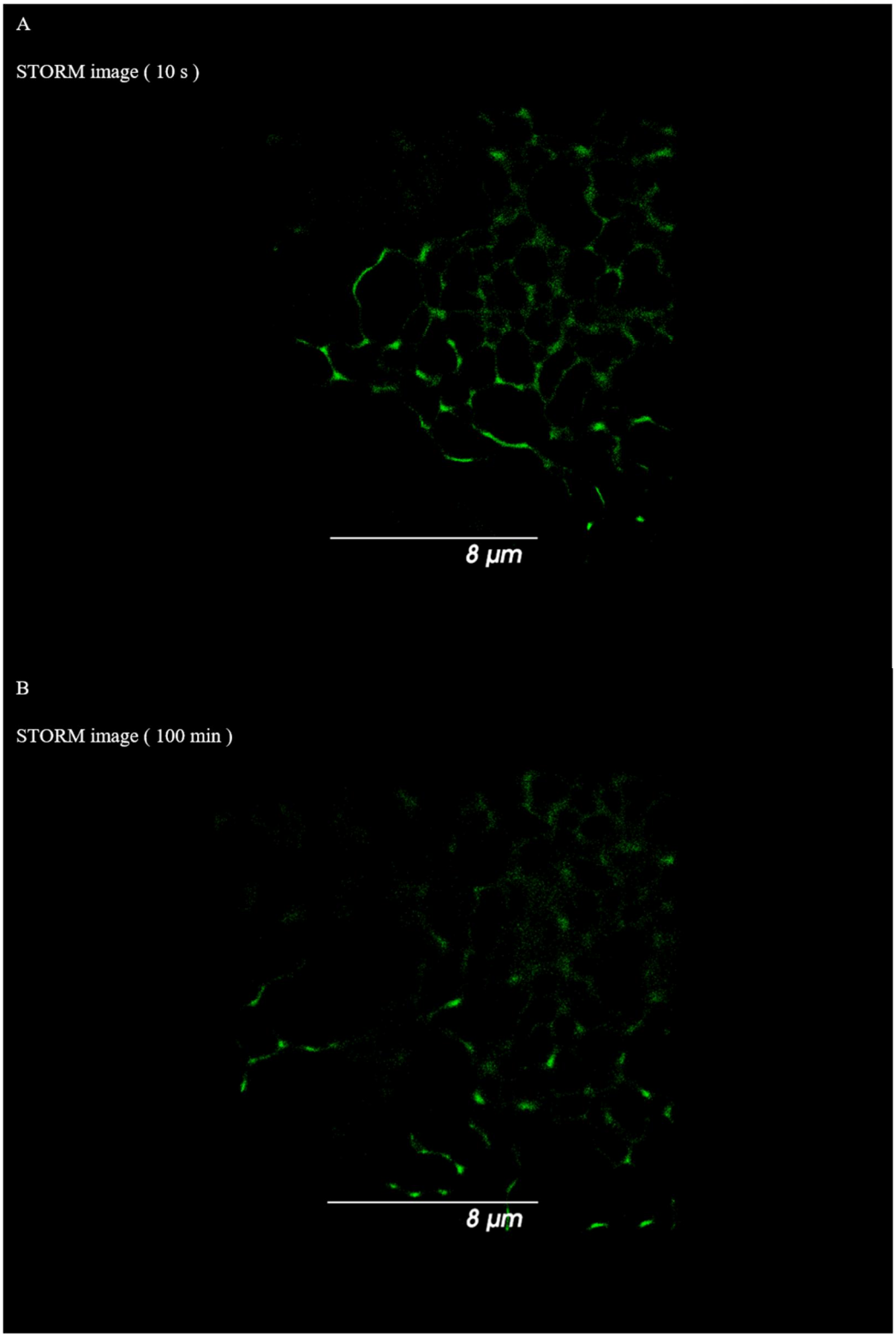

Figure 14. Long time-lapse STORM image of UnaG-sec61β.

(A) The first STORM image with 1000 frames of low level images. (B) STORM image composed of 1000 frames of low images after 100 minutes of continuous STORM imaging.

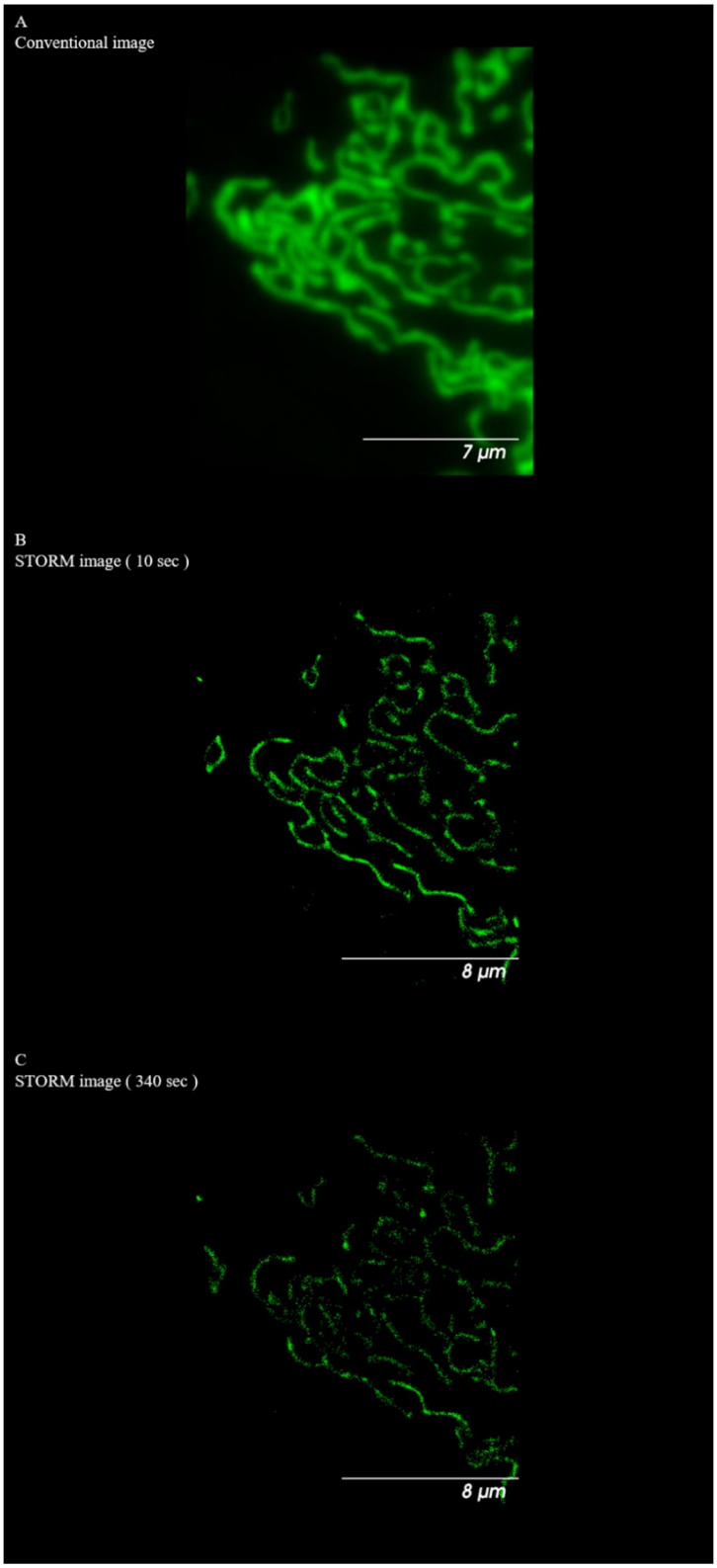

Figure 15. Long time-lapse STORM image of UnaG-mito.

(A) Conventional image before starting STORM imaging. (B) The First STORM image with 1000 frames of low images. (B) STORM image made with 1000 frames of low images at 300 seconds.

3.3. Two-Color (UnaG & Mitotracker Red) STORM Imaging

We also obtained two-color STORM images of the ER and mitochondria in live COS 7 cells (Fig. 16). ER was indicated with UnaG-sec61β and mitochondria was labeled with Mitotracker Red. Imaging was under simultaneous illumination of 488 nm laser and 561 nm laser. 488 nm laser was for UnaG excitation and 561 nm was for Mitotracker Red excitation. Imaging condition was same with single color STORM imaging. In this condition had challenge that imaging condition was suitable for UnaG but not for other dyes so that it is hard to obtain two-color imaging with UnaG and other organic dyes for STORM.

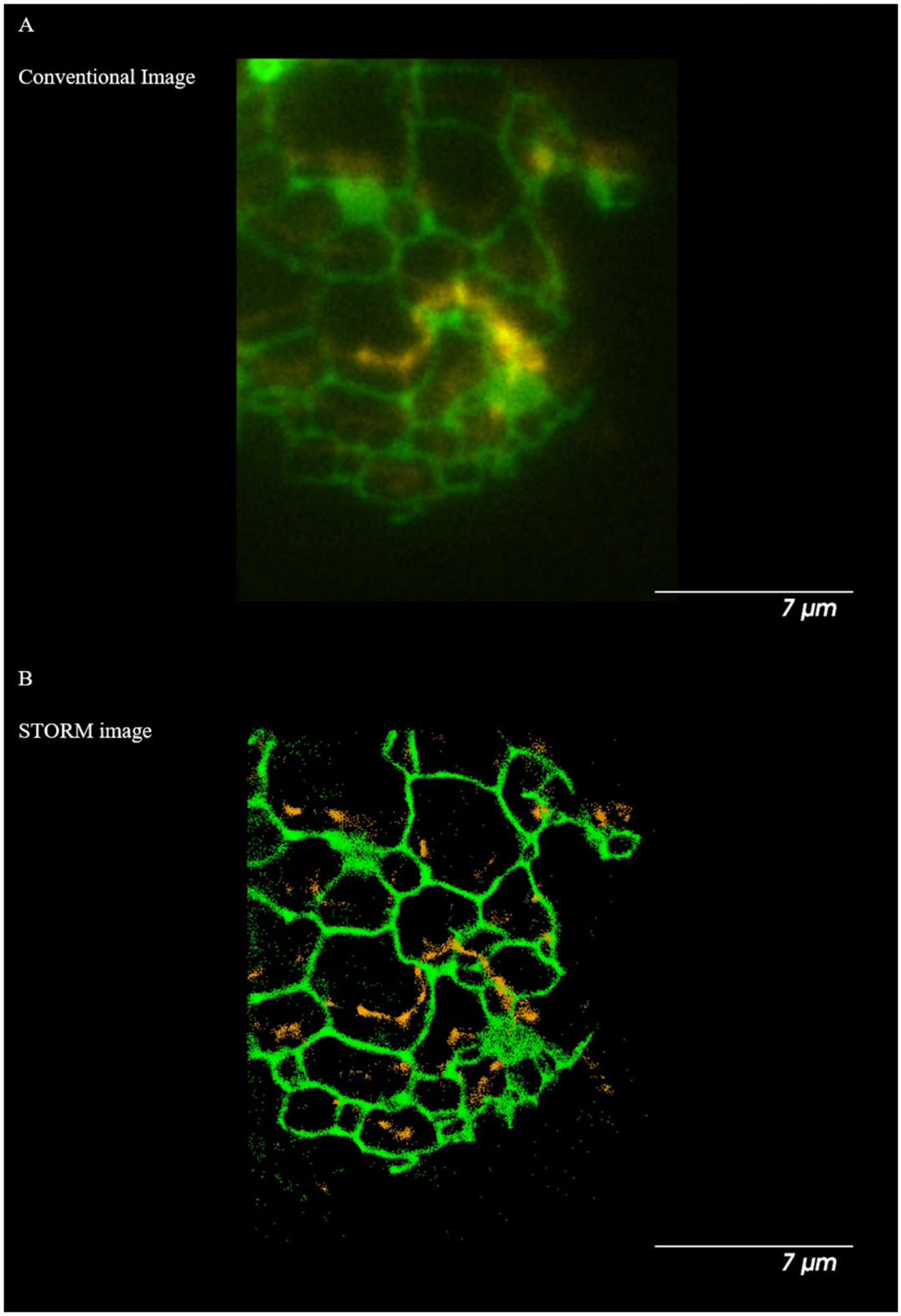

Figure 16. Two-Color STORM image.

(A) Conventional image and (B) STORM image of ER (UnaG) and mitochondria (Mitotracker Red). Scale bar is 7 μm

. Conclusion & Discussion

Live cell membranes exhibit pretty high dynamic motion. Super-resolution provides nanometer scale in cells and has been revealed ultrastructural information of many organelles. However, it has been hard to obtain time-lapse super-resolution images and main cause is photobleaching of dyes. UnaG could provide ideally no-photobleaching imaging tool for optical imaging with bilirubin addition. Also UnaG requires low laser intensity to switching. Therefore, we could approach to obtaining ultrastructural dynamics of cell with super-resolution imaging with UnaG construct. In this study, we studied various targeted STORM imaging with UnaG and tried to find proper STORM imaging condition especially for long time-lapse imaging. Because apoUnaG (non-fluorescenct form) could bind with fresh bilirubin, fluorescence of UnaG recovers its fluorescence by using nearby bilirubin. Also theoretically photobleaching might not occur in ideal case. However, usage of bilirubin could be harmful to cell because of its toxicity. Also to perform long time-lapse STORM imaging, it need to equip the circulation system of imaging buffer. Because exogenous bilirubin will be depleted and then photobleaching will occur, removing of oxidized bilirubin and supplementing of fresh bilirubin are needed to perform long time-lapse imaging.

The multi-color super-resolution imaging are needed to study interaction of various structures[20]. With UnaG, the multi-color STORM could be possible. But current STORM dyes are sensitive to the imaging buffer condition. It is needed to find the proper imaging condition satisfying UnaG and other dyes to perform long time-lapse STORM imaging.

. References

1. Rust, M.J., Bates, M. and Zhuang, X., 2006. Sub-diffraction-limit imaging by stochastic optical reconstruction microscopy (STORM). *Nature methods*, *3*(10), pp.793-796.

2. Gustafsson, M.G., 2005. Nonlinear structured-illumination microscopy: wide-field fluorescence imaging with theoretically unlimited resolution. *Proceedings of the National Academy of Sciences of the United States of America*, *102*(37), pp.13081-13086.

3. Willig, K.I., Rizzoli, S.O., Westphal, V., Jahn, R. and Hell, S.W., 2006. STED microscopy reveals that synaptotagmin remains clustered after synaptic vesicle exocytosis. *Nature*, *440*(7086), pp.935-939.

4. Betzig, E., Patterson, G.H., Sougrat, R., Lindwasser, O.W., Olenych, S., Bonifacino, J.S., Davidson, M.W., Lippincott-Schwartz, J. and Hess, H.F., 2006. Imaging intracellular fluorescent proteins at nanometer resolution. *Science*, *313*(5793), pp.1642-1645.

5. Huang, B., Babcock, H. and Zhuang, X., 2010. Breaking the diffraction barrier: super-resolution imaging of cells. *Cell*, *143*(7), pp.1047-1058.

6. Shim, S.H., Xia, C., Zhong, G., Babcock, H.P., Vaughan, J.C., Huang, B., Wang, X., Xu, C., Bi, G.Q. and Zhuang, X., 2012. Super-resolution fluorescence imaging of organelles in live cells with photoswitchable membrane probes. *Proceedings of the National Academy of Sciences*, *109*(35), pp.13978-13983.

7. Friedman, J.R., Lackner, L.L., West, M., DiBenedetto, J.R., Nunnari, J. and Voeltz, G.K., 2011. ER tubules mark sites of mitochondrial division. *Science*, *334*(6054), pp.358-362.

8. Dempsey, G.T., Vaughan, J.C., Chen, K.H., Bates, M. and Zhuang, X., 2011. Evaluation of fluorophores for optimal performance in localization-based super-resolution imaging. *Nature methods*, *8*(12), pp.1027-1036.

9. Subach, F.V., Patterson, G.H., Manley, S., Gillette, J.M., Lippincott-Schwartz, J. and Verkhusha, V.V., 2009. Photoactivatable mCherry for high-resolution two-color fluorescence microscopy. *Nature methods*, *6*(2), pp.153-159.

10. Bates, M., Huang, B., Dempsey, G.T. and Zhuang, X., 2007. Multicolor super-resolution imaging with photo-switchable fluorescent probes. *Science*, *317*(5845), pp.1749-1753.

11. Fernández-Suárez, M. and Ting, A.Y., 2008. Fluorescent probes for super-resolution imaging in living cells. *Nature Reviews Molecular Cell Biology*, *9*(12), pp.929-943.

12. Kumagai, A., Ando, R., Miyatake, H., Greimel, P., Kobayashi, T., Hirabayashi, Y., Shimogori, T. and Miyawaki, A., 2013. A bilirubin-inducible fluorescent protein from eel muscle. *Cell*, *153*(7), pp.1602-1611.

13. Park, J.S., Nam, E., Lee, H.K., Lim, M.H. and Rhee, H.W., 2016. In Cellulo Mapping of Subcellular Localized Bilirubin. *ACS chemical biology*.

14. Berry, C.S., Zarembo, J.E. and Ostrow, J.D., 1972. Evidence for conversion of bilirubin to dihydroxyl derivatives in the Gunn rat. *Biochemical and biophysical research communications*, *49*(5), pp.1366-1375.

15. Lippincott-Schwartz, J. and Patterson, G.H., 2009. Photoactivatable fluorescent proteins for diffraction-limited and super-resolution imaging. *Trends in cell biology*, *19*(11), pp.555-565.

16. McKinney, S.A., Murphy, C.S., Hazelwood, K.L., Davidson, M.W. and Looger, L.L., 2009. A bright and photostable photoconvertible fluorescent protein for fusion tags. *Nature methods*, *6*(2), p.131.

17. Biteen, J.S., Thompson, M.A., Tselentis, N.K., Bowman, G.R., Shapiro, L. and Moerner, W.E., 2008. Super-resolution imaging in live Caulobacter crescentus cells using photoswitchable EYFP. *Nature methods*, *5*(11), pp.947-949.

18. Patterson, G.H. and Lippincott-Schwartz, J., 2002. A photoactivatable GFP for selective photolabeling of proteins and cells. *Science*, *297*(5588), pp.1873-1877.

19. Dong, B., Yang, X., Zhu, S., Bassham, D.C. and Fang, N., 2015. Stochastic Optical Reconstruction Microscopy Imaging of Microtubule Arrays in Intact Arabidopsis thaliana Seedling Roots. *Scientific reports*, *5*.

20. Shroff, H., Galbraith, C.G., Galbraith, J.A. and Betzig, E., 2008. Live-cell photoactivated localization microscopy of nanoscale adhesion dynamics. *Nature methods*, *5*(5), pp.417-423.

Acknowledge

대학원 생활을 잘 지도 해 주신 배성철 교수님께 감사드립니다. 그리고 실험을 같이 진행하여 주신 UNIST 화학과 박종석 학생과 좋은 지도를 해주신 고려대학교 심상희 교수님, UNIST 화학과 이현우 교수님께도 감사드립니다. 2년 동안 실험실에서 잘 지낼 수 있게 도와주신 LABEL 실험실 사람들에게도 감사의 말씀을 전합니다. 무엇보다 뒤에서 묵묵히 지원해주신 부모님께 감사의 말씀을 드리고 싶습니다.